

---

# Tunable ballistic rectification in a density-modulated two-dimensional-system

A. GANCZARCZYK<sup>1</sup>, C. NOTTHOFF<sup>1</sup>, M. GELLER<sup>1</sup>, A. LORKE<sup>1</sup>, D. REUTER<sup>2</sup> and A. D. WIECK<sup>2</sup>

<sup>1</sup> *Laboratorium für Festkörperphysik und CeNIDE, Universität Duisburg-Essen, Lotharstraße 1, 47048 Duisburg, Germany*

<sup>2</sup> *Lehrstuhl für Angewandte Festkörperphysik, Ruhr-Universität Bochum, Universitätsstraße 150, 44780 Bochum, Germany*

PACS 73.23.Ad – Ballistic transport

PACS 73.40.Ei – Rectification

**Abstract.** - We demonstrate tunable rectification in a density-modulated two-dimensional electron gas (2DEG). The density modulation is induced by two surface gates, running in parallel along a narrow strip of 2DEG. A transverse voltage in the direction of the density-gradient is observed, i.e. perpendicular to the applied source-drain voltage. The transverse voltage depends on the sign and magnitude of the density gradient. The polarity of the transverse voltage is independent of the polarity of the source-drain voltage demonstrating rectification in the device. The experimental results are discussed in the framework of a classical, single particle billiard model.

---

The high charge carrier mobilities of two-dimensional electron gases (2DEGs) in semiconductor heterostructures combined with lithography on the nanometer scale have made it possible to study ballistic transport in semiconductor devices with feature sizes smaller than the elastic mean free path. In such mesoscopic devices, certain transport properties are determined by the geometry of the device rather than by material properties. In these structures with ballistic transport, nonlinear behaviour can be observed, such as bend resistance in mesoscopic cross structures [1, 2] or symmetric behaviour of two-terminal nonlinear electric conduction [3]. It has been reported that such devices can operate up to room-temperature and at switching frequencies of more than 50 GHz [4]. Other examples are three-terminal ballistic Y switches [5–7], or ballistic rectifiers of different designs [8–12].

In the past, the ballistic rectification in such devices has been obtained by the broken symmetry in the shape of a mesoscopic cross junction. In the first example of a ballistic rectifier by Song et al. [8], the symmetry breaking structure consists of an asymmetric artificial scatterer in the shape of a triangle. The scatterer guides carriers in a predetermined spatial direction, independent of the direction of the input current. Here, we will investigate whether rectification can be obtained, when the broken symmetry is caused by a step in the carrier density parallel to the input current. The idea for this arrangement derives itself

from the question whether a broken symmetry between "left" and "right" can lead to a net flow between left and right for non-equilibrium electrons. While Song et al. used specular reflection of electrons to achieve the rectification, we use the refraction of electrons at the density-step in the 2DEG according to Snell's law for charge carrier densities. Manipulation of ballistic electrons by refraction was successfully used before in the linear regime [13–16]. To the best of our knowledge, however, the nonlinear properties of refraction in ballistic semiconductor structures have not been studied before.

We here present a new device geometry to build a ballistic electron rectifier, in which the sign and the amplitude of the rectified voltage can be tuned by an applied gate voltage. The rectifying device consists of a long, narrow two-dimensional conductive channel, partially covered by two parallel metallic surface gate electrodes (see fig. 1). By applying a voltage to the two gates, we induce two stripes of different charge carrier densities running parallel to the channel. When a current is applied along the channel, the density gradient perpendicular to the channel induces a transverse voltage, which - due to the symmetry of the device - does not change polarity when the current direction is reversed. The results are reproduced by a classical, single particle billiard model [17], which describes the motion of ballistic electrons.

The samples investigated here, are fabricated from a

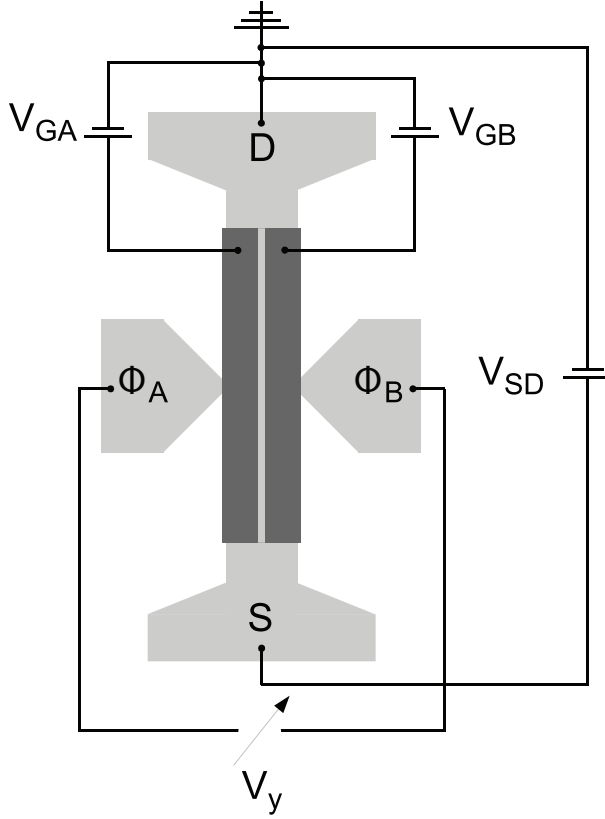


Fig. 1: Schematic picture of the rectifier and the experimental setup. The source-drain voltage  $V_{SD}$  and the gate voltages  $V_{GA}$  and  $V_{GB}$  are both referenced to the drain terminal.  $\Phi_A$  and  $\Phi_B$  are the potentials at  $A$  and  $B$ , respectively. The transverse voltage  $V_y$  is measured between  $A$  and  $B$ , and  $V_y$  is defined as  $V_y = \Phi_B - \Phi_A$ . The 2DEG defined by an etched mesa is indicated in light grey, the metallic gate electrodes in dark grey.

modulation-doped GaAs/Al<sub>0.34</sub>Ga<sub>0.66</sub>As heterostructure grown by molecular beam epitaxy. The heterostructure contains a 2DEG, situated 110 nm below the surface. The sheet charge carrier density, mobility and mean free path at a temperature of  $T = 4.2$  K are  $2.87 \cdot 10^{15} \text{ m}^{-2}$ ,  $28.8 \text{ m}^2/\text{Vs}$  and  $\approx 5 \mu\text{m}$ , respectively. Optical lithography and successive wet chemical etching is used to define the macroscopic mesa structure. Ohmic contacts are made of Ni/AuGe/Au layers formed by high-vacuum deposition and successive thermal annealing. The metallic gate electrodes are defined by electron beam lithography and consist of a 50 nm thick Au layer. A schematic picture of the rectifier is shown in fig. 1. The source-drain voltage  $V_{SD}$  is applied between the "S" and "D" terminals. Different gate voltages  $V_{GA}$ ,  $V_{GB}$  can be applied to the gates. The transverse voltage  $V_y$  is measured between the terminals  $A$  and  $B$ . The conductive channel has a length of  $1000 \mu\text{m}$  and a width of  $100 \mu\text{m}$ , while the length of the two metallic gate electrodes is  $900 \mu\text{m}$  and the distance between the two gates is  $1 \mu\text{m}$ , which equals the width of the transition region between areas of different carrier densities. While the overall sample size

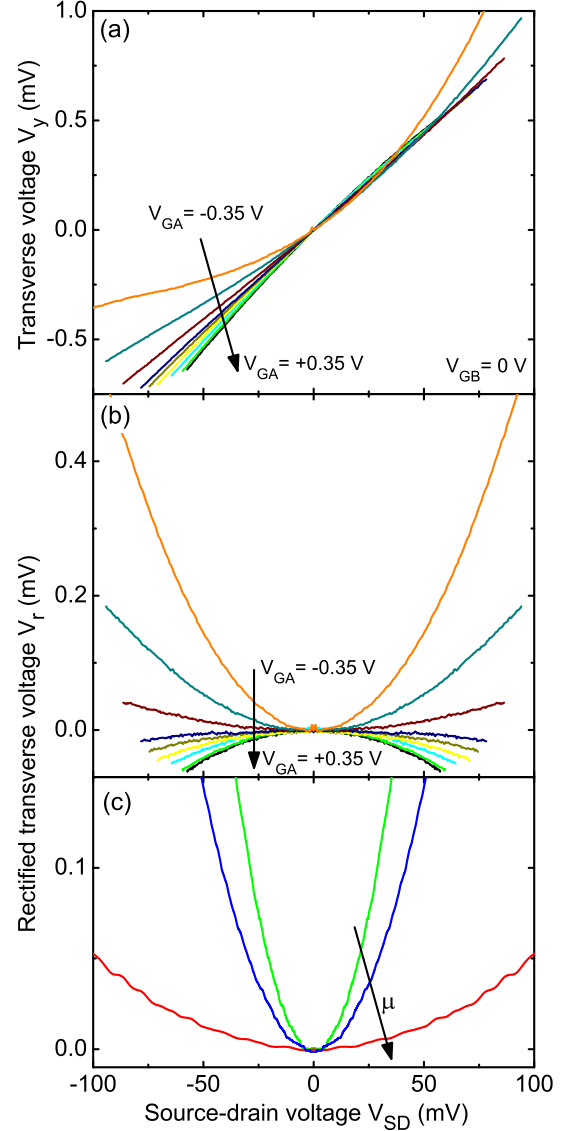


Fig. 2: (a): Dependence of the transverse voltage  $V_y$  on the source-drain voltage  $V_{SD}$ . The gate voltage  $V_{GA}$  is applied from  $+0.35$  V (black trace) to  $-0.35$  V (orange trace) in steps of  $0.1$  V. The dark green trace shows the transverse voltage for  $V_{GA} = 0$  V. (b): Symmetric contribution of the transverse voltage  $V_r$  as a function of the source-drain voltage  $V_{SD}$ . (c): Influence of the carrier mobility on the transverse voltage. The red and blue traces show  $V_r$  for  $77$  K (mobility  $10 \text{ m}^2/\text{Vs}$ ) and  $4.2$  K (mobility  $29 \text{ m}^2/\text{Vs}$ ), respectively. The green trace shows  $V_r$  for a device fabricated from a different heterostructure (mobility  $50 \text{ m}^2/\text{Vs}$ , carrier density  $4.5 \cdot 10^{15} \text{ m}^{-2}$  at  $4.2$  K). The output voltage increases with increasing mobility.

is much higher than the mean free path, the dimension of the most important part in the sample, namely the transition region, is much smaller. Using a macroscopic sample geometry enables us to use source-drain voltages in the order of  $100$  mV without occupation of excited subbands

in the 2DEG and ensures a homogeneous current flow. All measurements are performed at 4.2 K.

Figure 2(a) shows the transverse voltage  $V_y$  as a function of the source-drain voltage  $V_{SD}$  for different gate voltages  $V_{GA}$ . In the following,  $V_{GA}$  is applied between gate A and ground, whereas gate B is always grounded, so in effect, two parallel stripes of different carrier density are formed. Similar results have been obtained using a 'push-pull' configuration, applying  $V_{SD}$  symmetrically with respect to the middle terminals [12]. Note that in order to maintain the full symmetry of the device along the current direction, two identical gates were prepared. This also allows us to also realize device configurations with three stripes of different carrier densities. For reasons of clarity, however, we only show measurements with one gate biased. The measurements taken with both gates biased show the same characteristics as the data discussed here.

It can be seen that  $V_y$  is dominated by a contribution, which depends roughly linearly on  $V_{SD}$ . We attribute this linear antisymmetric contribution to imperfections of the device geometry such as slightly shifted voltage probes and a minute misalignment angle between the gates and the etched channel. Symmetry considerations show that such contributions are antisymmetric with respect to  $V_{SD}$ , whereas all contributions originating from the two parallel stripes of different carrier density must be symmetric in  $V_{SD}$ . A separation of the symmetric part  $V_r = [V_y(V_{SD}) + V_y(-V_{SD})]/2$  yields the rectification characteristics, which will be discussed in the following. Note, however, that a rectifying behaviour can already be seen in the raw data in fig. 2, in particular for  $V_{GA} = -0.35$  V.

The symmetric part of the transverse voltage  $V_r$  shown in fig. 2(b) exhibits a parabolic dependence on the source-drain voltage  $V_{SD}$ . Somewhat surprisingly, we find  $V_r \propto V_{SD}^2$  to an accuracy of about  $10^{-3}$ . Increasing the source-drain voltage  $V_{SD}$  to 100 mV leads to a transverse voltage  $V_r$  of 0.58 mV for a gate voltage of  $V_{GA} = -350$  mV. The polarity of the rectified transverse voltage  $V_r$  depends only on the polarity of the gate voltages and corresponds to an induced flow of electrons from the high-carrier-density area to the low-density-area. Furthermore, the measurements demonstrate that the value of the transverse voltage depends on the magnitude of the density-gradient (increasing transverse voltage with increasing difference in the gate voltages, fig. 2(b)) and on the charge carrier mobility, fig. 2(c).

To account for the experimental results, we numerically simulate the "refraction" of ballistic electrons at the boundary between areas of different charge carrier densities (see inset fig. 3 using Snell's law for charge carrier densities [13–16]). The simulation includes the electric field needed to drive the applied source-drain current. This is an essential ingredient, since no charge separation is possible for a system in equilibrium. All electrons start at the source terminal with randomly chosen starting angle. After a random scattering time - chosen with a Possionian distribution - a new random angle is set for each electron.

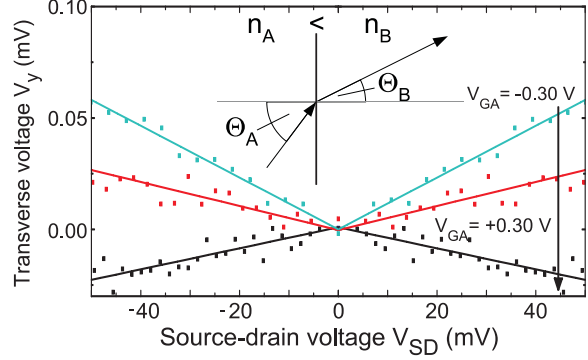


Fig. 3: Calculated transverse voltage  $V_y$  as a function of the source-drain voltage  $V_{SD}$  for different gate voltages  $V_{GA} = -0.30$  V,  $-0.15$  V,  $+0.30$  V. Note that, because no distinction between positive and negative bias is possible in the simulation, any resulting output voltage  $V_y$  must be identical for both polarities of  $V_{SD}$ . The data points represent the simulated transverse voltage, the lines are the modulus fits to the numerical results. The inset schematically shows the refraction of an electron at a boundary separating two regions of different electron densities.

Between scattering events, the electrons move ballistically under the influence of refraction and acceleration by the source-drain field. This process is repeated until the electron reaches the drain terminal<sup>1</sup>. The number of electrons starting from the regions A and B at the source terminal is chosen according to the respective carrier densities in the 2DEG. The corresponding numbers at the drain terminal are evaluated from the simulation. The relative change in population is converted into a change in Fermi-energy, which is then converted into a built in (transverse) voltage. To check the validity of the procedure and to avoid numerical artifacts, we calculated the transverse voltage in the absence of a driving source-drain bias and found an almost vanishing transverse voltage, as expected for the equilibrium situation. Furthermore, we verified that the calculated transverse voltage is independent of the source-drain distance and thus represents the steady-state value.

Figure 3 shows the simulated transverse voltage  $V_y$  as a function of the source-drain voltage  $V_{SD}$  for different gate voltages  $V_{GA}$ . The data points represent the numerical results, whereas the lines are the modulus function fits to the data points. For negative gate voltages  $V_{GA}$ , the transverse voltage  $V_y$  is positive ( $\Phi_A < \Phi_B$ ). The opposite polarity is observed for positive gate voltages. The same behaviour is observed in the measurements, where the transverse current also corresponds to a flow of electrons towards the lower density area. The simulation also shows similar dependences on the magnitude of the density-gradient and on the carrier mobility as in the measurements. Furthermore, both experimental and

<sup>1</sup>To ensure that the electrons reach the drain terminal after a manageable number of scattering events, only forward scattering (scattering angle  $-\frac{\pi}{2} < \Theta_{sc} < \frac{\pi}{2}$ ) is taken into account.

simulated results yield transverse voltages in the same order of magnitude (between 5 and 25  $\mu\text{V}$ ) for source-drain voltages up to  $V_{SD} \approx 25$  mV. However, the dependence of the calculated transverse voltage on the source-drain voltage resembles a modulus function ( $V_r \propto |V_{SD}|$ , i.e. nonlinear/non-ohmic), whereas the experiment shows a parabolic dependence. This indicates that the presence of the transverse voltage cannot be fully described with the model developed here. More sophisticated transport models need to be developed to explain this discrepancy.

The numerical simulations clearly indicate that the observed rectification can be traced back to the ballistic motion in the vicinity of the density gradient. This is further supported by the dependence of the rectified voltage on the electronic mean free path, given by the 2DEG mobility. As shown in fig. 2(c), changing the carrier mobility by either changing the temperature or using a different heterostructure, strongly influences the rectified voltage. In agreement with the ballistic picture,  $V_r$  increases with increasing mobility. Furthermore, thermoelectric effects [18] can be ruled out as a possible explanation for the observed rectification because of the constant density of states in 2DEGs. Using the analytical expression given by Davies [19,20] for the chemical potential as a function of temperature, we estimate the thermal voltage in the present experiment to be the order of  $10^{-12}$  V.

We would like to mention that even though the above discussion is based on the physics of ballistic rectifiers, our results could have much broader significance. For example, the two metallic regions with different carrier densities do not necessarily have to be two-dimensional. Also, the structure is essentially featureless along the direction of the input current (contrary to other ballistic rectification devices). It is therefore possible to realize a corresponding three-dimensional structure by simply fusing or evaporating two metals of different carrier density. In general, our findings may be of relevance for other binary systems, where the non-equilibrium scattering at the boundary is symmetry-broken. A periodic continuation of the density gradient, while keeping the broken symmetry in  $y$ -direction, would lead to a ratchet potential. In such a ratchet, an agitation along the  $x$ -direction would induce a net flow of carriers perpendicular to the direction of excitation. First experiments to realize such a 'transverse ratchet' are presently under way.

In conclusion, we have demonstrated tunable ballistic rectification in a density-modulated two-dimensional system. The polarity and value of the rectified transverse voltage depend on the direction and magnitude of the density gradient of the charge carrier density inside the 2DEG. The results are partially in agreement with a simulation based on a classical billiard model. While the experiment results show a quadratic dependence of the transverse voltage on the source-drain voltage, the results from the simulation give a behavior, which resembles a modulus function. The calculated data reproduces the correct output polarity of the transverse voltage, the qualitative

dependence of transverse voltage on the gate voltage and the observation that the transverse voltage increases with increasing mobility.

\* \* \*

We thank Alik Chaplik and Dietrich Wolf for very fruitful discussions and acknowledge financial support from the SFB 616.

## REFERENCES

- [1] TIMP G., BARANGER H. U., DEVEGVAR P., CUNNINGHAM J. E., HOWARD R. E., BEHRINGER R. and MANKIEWICH P. M., *Phys. Rev. Lett.* , **60** (1988) 2081.
- [2] HIRAYAMA Y., SAKU T., TARUCHA S. and HORIKOSHI Y., *Appl. Phys. Lett.* , **58** (1991) 2672.
- [3] LOFGREN A., MARLOW C. A., SHORUBALCO I., TAYLOR R. P., OMLING P., SAMUELSON L. and LINKE H., *Phys. Rev. Lett.* , **92** (2004) 046803.
- [4] SONG A. M., OMLING P., SAMUELSON L., SEIFERT W., SHORUBALCO I. and ZIRATH H., *Appl. Phys. Lett.* , **79** (2001) 1357.
- [5] HIEKE K. and ULFWARD M., *Phys. Rev. B* , **62** (2000) 16727.
- [6] WORSCHER L., WEIDNER B., REITZENSTEIN S. and FORCHEL A., *Appl. Phys. Lett.* , **78** (2001) 3325.
- [7] XU H. Q., *Appl. Phys. Lett.* , **78** (2001) 2064.
- [8] SONG A. M., LORKE A., KRIELE A., KOTTHAUS J. P., WEGSCHEIDER W. and BICHLER M., *Phys. Rev. Lett.* , **80** (1998) 3831.
- [9] LOFGREN A., SHORUBALCO I., OMLING P. and SONG A. M., *Phys. Rev. B* , **67** (2003) 195309.
- [10] HACKENS B., GENCE L., GUSTIN C., WALLART X., BOLLAERT S., CAPPY A. and BAYOT V., *Appl. Phys. Lett.* , **85** (2004) 4508.
- [11] DE HAAN S., LORKE A., KOTTHAUS J. P., WEGSCHEIDER W. and BICHLER M., *Phys. Rev. Lett.* , **92** (2004) 56806.
- [12] KNOP M., WIESER U., KUNZE U., REUTER D. and WIECK A. D., *Appl. Phys. Lett.* , **88** (2006) 082110.
- [13] SPECTOR J., STORMER H. L., BALDWIN K. W., PFEIFFER L. N. and WEST K. W., *Appl. Phys. Lett.* , **56** (1990) 2433.
- [14] SPECTOR J., STORMER H. L., BALDWIN K. W., PFEIFFER L. N. and WEST K. W., *Appl. Phys. Lett.* , **56** (1990) 1290.
- [15] NOGUCHI M., SAKAKIBARA H. and IKOMA T., *Jpn. J. Appl. Phys.* , **32** (1993) 5014.
- [16] FUKAI Y. K., TARUCHA S., HIRAYAMA Y., TOKURA Y. and SAKU T., *Appl. Phys. Lett.* , **60** (1992) 106.
- [17] BEENAKKER C. W. J. and VAN HOUTEN H., *Phys. Rev. Lett.* , **63** (1989) 1857.
- [18] MOLENKAMP L. W., VAN HOUTEN H., BEENAKKER C. W. J., EPPENGA R. and FOXON C. T., *Phys. Rev. Lett.* , **65** (1990) 1052.
- [19] DAVIES J. H., *The Physics of Low-Dimensional Semiconductors* (Cambridge University Press, Cambridge) 1998.
- [20] ASHCROFT N. W. and MERMIN I., *Solid State Physics* (Saunders College Company, Philadelphia) 1976.